PHASE UNWRAPPING: A NEW MAX-FLOW/MIN-CUT BASED APPROACH

José M. Bioucas-Dias

IT, Instituto Superior Técnico,
Torre Norte, Piso 10,
Av. Rovisco Pais,
1049-001 Lisboa, PORTUGAL
Email: bioucas@lx.it.pt

Gonçalo Valadão

ICIST, Instituto Superior Técnico,
Departamento de Engenharia Civil
Av. Rovisco Pais,
1049-001 Lisboa, PORTUGAL
Email: gvm@civil.ist.utl.pt

ABSTRACT

The paper presents a new max-flow/min-cut approach for recovering the absolute phase from modulo-2π phase, the so-called phase unwrapping (PU) problem. The adopted criterion is the minimization of the L^p norm of phase differences, leading to computationally demanding integer optimization problems. The unwrapped phase is computed iteratively through a sequence of binary optimizations, each one mapped onto a max-flow/min-cut problem on a certain graph. Accordingly, we name this new algorithm PUMF (for phase unwrapping max-flow). A set of experimental results illustrates the effectiveness of PUMF approach, namely for $0 < p < 1$, where most competitors fail.

1. INTRODUCTION

Phase is an important feature of many signal/image applications [1]. For instance, interferometric SAR (InSAR) uses two or more antennas to measure the phase between the antennas and the terrain; the topography is then inferred from the difference between those phases [2]. In magnetic resonance imaging (MRI), phase is used, namely, to determine magnetic field deviation maps, which are used to correct echo-planar image geometric distortions [3]. In optical interferometry, phase measurements are used to detect objects shape, deformation, and vibration [4].

In all the examples above, the acquisition system can only measure phase modulo-2π, the so-called *principal phase value*, or *wrapped phase*. Formally, we have

$$\phi = \psi + 2k\pi, \tag{1}$$

where ϕ is the true phase value (the so-called *absolute value*), ψ is the measured (wrapped) modulo-2π phase value, and $k \in \mathbb{Z}$ an integer number of wavelengths [1].

Phase unwrapping (PU) is the process of recovering the absolute phase ϕ from the wrapped phase ψ. This is, however, an ill-posed problem, if no further information is added. In fact, an assumption taken by most phase unwrapping methodologies is that the absolute value of phase differences between neighboring pixels is less than π, the so-called Itoh condition [5]. If this assumption is not violated, the absolute phase can be easily determined, up to a constant. Itoh condition might be violated if the true phase surface is discontinuous, or if only a noisy version of the wrapped phase is available. In either cases, PU becomes a very difficult problem, to which much attention has been devoted (see, e.g., [1], [6]).

This work was supported by the Fundação para a Ciência e Tecnologia, under the project PDCTE/CPS/49967/2004.

Phase unwrapping approaches belong to one of the following classes: path following [7], minimum L^p norm [8], Bayesian [9], and parametric modeling [10].

Path following algorithms apply line integration schemes over the wrapped phase image, and basically rely on the assumption that Itoh condition holds along the integration path. Wherever this condition is not met, different integration paths may lead to different unwrapped phase values. Techniques employed to handle these inconsistencies include the so-called *residues branch cuts* [7] and *quality maps* [1].

If Itoh condition is met, the absolute phase difference of neighboring pixels is equal to the correspondent wrapped phase difference; minimum norm methods exploit this fact, by finding a phase solution ϕ for which the L^p norm of the above difference is minimized. This is, therefore, a batch minimization scheme. With $p = 2$ we have a least squares method [11]. The exact solution with $p = 2$ is developed in [6] using network programming techniques. An approximation to the least squares solution can be obtained by relaxing the discrete domain $\mathbb{Z}^{MN}$ to $\mathbb{R}^{MN}$ and applying FFT or DCT based techniques[1]. A drawback of the L^2 norm is that this criterion tends to smooth discontinuities, unless they are provided as binary weights. L^1 norm performs better in what discontinuity preserving is concerned. Such a criterion has been solved by Flynn [12] and Costantini [13], using network programming methods. With $0 \leq p < 1$ the ability of preserving discontinuities is further increased at stake, however, of highly complex algorithms.

The Bayesian approach relies on a data-observation mechanism model, as well as a prior knowledge of the phase to be modeled. For instance, work [14] considers non-linear observation models with Markov Random Field priors.

Finally, parametric algorithms constrain the unwrapped phase to a parametric surface. Low order polynomial surfaces are used in [10]. Very often in real applications just one polynomial is not enough to describe accurately the complete surface. In such cases the image is partitioned and different parametric models are applied to each partition [10].

1.1. Proposed approach

This paper extends the L^p norm concept applied to PU and introduces a new optimization scheme. The integer optimization problem we are led to is solved by a series of binary elementary optimizations as presented in [6] for the $\mathbb{Z}\pi$M algorithm. The present approach casts the optimization problem into a sequence of max-flow/min-cut calculations on a certain graph, building on energy minimization

[1] M and N are the number of lines and columns respectively.

results presented in [15]. Accordingly we call the method to be presented the PUMF algorithm (for PU and max-flow).

We show that for $p \geq 1$ the algorithm computes the exact solution. For $0 < p < 1$, the problem at hand is NP-hard [16]. Nevertheless, in a series of difficult benchmark examples, where state-of-the-art competitors fail, the underlaying surfaces were effectively unwrapped.

2. PROBLEM FORMULATION

Let ϕ_{ij} denote the phase to be reconstructed at pixel (i,j). The L^p norm of the difference between neighboring pixels phases, 2π-congruent with wrapped phases, is given by

$$E(\mathbf{k}|\boldsymbol{\psi}) = \sum_{ij\in\mathbb{Z}_1} \left|\Delta\phi_{ij}^h\right|^p \overline{v}_{ij} + \left|\Delta\phi_{ij}^v\right|^p \overline{h}_{ij}, \qquad (2)$$

where $(\cdot)^h$ and $(\cdot)^v$ denotes pixel horizontal and vertical differences given by

$$\Delta\phi_{ij}^h = \left[2\pi(k_{ij} - k_{ij-1}) - \Delta\psi_{ij}^h\right],\ k \in \mathbb{Z} \qquad (3)$$

$$\Delta\phi_{ij}^v = \left[2\pi(k_{ij} - k_{i-1j}) - \Delta\psi_{ij}^v\right],\ k \in \mathbb{Z} \qquad (4)$$

$$\Delta\psi_{ij}^h = \psi_{ij-1} - \psi_{ij} \qquad (5)$$

$$\Delta\psi_{ij}^v = \psi_{i-1j} - \psi_{ij}, \qquad (6)$$

with $p \geq 0$, ψ being the wrapped (observed) phase, $\overline{h}_{ij} = 1 - h_{ij}$ and $\overline{v}_{ij} = 1 - v_{ij}$ ($h_{ij}, v_{ij} \in \{0,1\}$) being binary horizontal and vertical discontinuities respectively, and $(i,j) \in \mathbb{Z}_1$ where $\mathbb{Z}_1 = \{(i,j) : i = 1,\dots,M,\ j = 1,\dots,N\}$, and whith M and N denoting the number of lines and columns respectively (i.e., the usual image pixel indexing 2D grid).

In PU literature, L^p norm has been defined similarly to (2), but with terms $\Delta\phi$ replaced with the 2π quantized version (see [12]). All the concepts and results herein presented are valid for both cases. In the exposition we proceed with the non-quantized L^p norm. Wherever we use the quantized version, explicit reference is made.

Our purpose is to find the integer image $\mathbf{k} \equiv \{k_{ij}\}$ that minimizes energy (2), $\mathbf{k}$ being such that $\boldsymbol{\phi} = 2\pi\mathbf{k} + \boldsymbol{\psi}$, where $\boldsymbol{\phi}$ is the estimated unwrapped image; $\mathbf{k}$ is the so-called *wrap-count* image. To achieve this goal, we cast this integer problem into a series of graph flow calculations for which efficient max-flow/min-cut algorithms exist.

3. ENERGY MINIMIZATION BY A SEQUENCE OF BINARY OPTIMIZATIONS

The following lemma, taken from [6], assures that if the minimum of $E(\mathbf{k}|\boldsymbol{\psi})$ is not yet reached, then there exists a binary image $\delta\mathbf{k}$ (i.e., the elements of $\delta\mathbf{k}$ are all 0 or 1) such that $E(\mathbf{k}+\delta\mathbf{k}|\boldsymbol{\psi}) < E(\mathbf{k}|\boldsymbol{\psi})$.

Lemma 1 *Let* $\mathbf{k}_1$ *and* $\mathbf{k}_2$ *be two wrap-count images such that*

$$E(\mathbf{k_2}|\boldsymbol{\psi}) < E(\mathbf{k_1}|\boldsymbol{\psi}). \qquad (7)$$

Then, if $p \geq 1$, *there exists a binary image* $\delta\mathbf{k}$ *such that*

$$E(\mathbf{k_1} + \delta\mathbf{k}|\boldsymbol{\psi}) < E(\mathbf{k_1}|\boldsymbol{\psi}). \qquad (8)$$

The proof follows the same line of Lemma 1 published in [6] for $p = 2$, using the convexity of $|x|^p$ with respect to x, for $p \geq 1$.

According to Lemma 1, we can iteratively compute $\mathbf{k}^{t+1} = \mathbf{k}^t + \delta\mathbf{k}$, where $\delta\mathbf{k} \equiv \{\delta k_{ij}\}$ and $\delta\mathbf{k} \in \{0,1\}^{MN}$ minimizes $E(\mathbf{k}^t + \delta\mathbf{k}|\boldsymbol{\psi})$, until the the minimum energy is reached.

3.1. Mapping Binary Optimizations onto Graph Min-Cuts

Let $k_{ij}^{t+1} = k_{ij}^t + \delta k_{ij}^t$ be the wrapp-count at time $t+1$ and pixel (i,j). Introducing k_{ij}^{t+1} into (3) and (4), we obtain, respectively,

$$\Delta\phi_{ij}^h = \left[2\pi(k_{ij}^{t+1} - k_{ij-1}^{t+1}) - \Delta\psi_{ij}^h\right] \qquad (9)$$

$$\Delta\phi_{ij}^v = \left[2\pi(k_{ij}^{t+1} - k_{i-1j}^{t+1}) - \Delta\psi_{ij}^v\right]. \qquad (10)$$

After some simple manipulation, we get

$$\Delta\phi_{ij}^h = \left[2\pi(\delta k_{ij}^t - \delta k_{ij-1}^t) + a^h\right] \qquad (11)$$

$$\Delta\phi_{ij}^v = \left[2\pi(\delta k_{ij}^t - \delta k_{i-1j}^t) + a^v\right], \qquad (12)$$

where

$$a^h = 2\pi(k_{ij}^t - k_{ij-1}^t) - \Delta\psi_{ij}^t \qquad (13)$$

$$a^v = 2\pi(k_{ij}^t - k_{i-1j}^t) - \Delta\psi_{ij}^t. \qquad (14)$$

Now introducing (11) and (12) into (2), we can rewrite energy $E(\mathbf{k}|\boldsymbol{\psi})$ as a function of binary variables δk_{ij}^t, i.e.,

$$\begin{aligned} E(\mathbf{k}|\boldsymbol{\psi}) &= \sum_{ij\in\mathbb{Z}_1} \underbrace{\left|2\pi(\delta k_{ij}^t - \delta k_{ij-1}^t) + a^h\right|^p \overline{v}_{ij}}_{E_h^{ij}(x_{ij-1},x_{ij})} \\ &+ \underbrace{\left|2\pi(\delta k_{ij}^t - \delta k_{i-1j}^t) + a^v\right|^p \overline{h}_{ij}}_{E_v^{ij}(x_{i-1j},x_{ij})}, \end{aligned} \qquad (15)$$

where $x_{ij} = \delta k_{ij}^t$.

For simplicity, let us denote for a moment terms E_h^{ij} and E_v^{ij} by $E^{ij}(x_k, x_l)$. We have thus,

$$\begin{aligned} E^{ij}(0,0) &= |a|^p\, \overline{d}_{ij}, \\ E^{ij}(1,1) &= |a|^p\, \overline{d}_{ij}, \\ E^{ij}(0,1) &= |2\pi + a|^p\, \overline{d}_{ij}, \\ E^{ij}(1,0) &= |-2\pi + a|^p\, \overline{d}_{ij}, \end{aligned}$$

where a represents a_h or a_v and $\overline{d}_{ij}$ represents $\overline{h}_{ij}$ or $\overline{v}_{ij}$.
So we have

$$E^{ij}(0,0) + E^{ij}(1,1) = 2\,|a|^p\, \overline{d}_{ij} \qquad (16)$$

and

$$E^{ij}(0,1) + E^{ij}(1,0) = \left(|-2\pi + a|^p + |2\pi + a|^p\right) \overline{d}_{ij}. \qquad (17)$$

For $p \geq 1$, terms $E(x_k, x_l)$ verify

$$E^{ij}(0,0) + E^{ij}(1,1) \leq E^{ij}(0,1) + E^{ij}(1,0), \qquad (18)$$

this following from the convexity of $E(\mathbf{k}|\boldsymbol{\psi})$.

According to [15], the inequality (18) assures that $E(\mathbf{k}|\boldsymbol{\psi})$ is *graph-representable*, i.e., there exists a one-to-one mapping between the configuration of $(x_1,\dots,x_n)$ and the cuts on a certain graph; furthermore, the cost of the cut is the value of the energy of that configuration. Therefore, minimizing the energy is equivalent to computing the max-flow/min-cut. The graph is constructed as follows (see [15]): first, build vertices and edges corresponding to each pair of neighboring pixels, and then join these graphs together based on the *additivity theorem* also given in [15]. For each energy term E_h^{ij} and E_v^{ij} (see expression (15)), we construct an *elementary* graph with four vertices $\{s,t,v,v'\}$, where $\{s,t\}$ represents source and the sink, common to all terms, and $\{v,v'\}$ represents the two pixels involved (v being the left (up) pixel and v' the right (down)

Algorithm 1 (PUMF) Graph cuts based phase unwrapping algorithm.

Initialization: $\boldsymbol{k}^{(0)} = \mathbf{0}$, possible_ improvement $\equiv 0$ {$\boldsymbol{k}^{(0)}$ is the initial **k** image}

while possible_improvement **do**
  Compute $E(0,0), E(1,1), E(0,1)$, and $E(1,0)$ {for every horizontal and vertical pixel pairs}.
  Construct elementary graphs and merge them to obtain the main graph.
  Compute the min-cut (S, T) {S- source set; T-sink set}.
  for all pixel (i, j) **do**
    if pixel $(i, j) \in S$ **then**
      $\boldsymbol{k}_{i,j} = \boldsymbol{k}_{i,j} + 1$
    else
      $\boldsymbol{k}_{i,j} = \boldsymbol{k}_{i,j}$ {remains unchanged}
    end if
  end for
end while

pixel). Following very closely [15], we define a directed edge (v, v') with the weight $E(0,1) + E(1,0) - E(0,0) - E(1,1)$. Moreover, if $E(1,0) - E(0,0) > 0$ we define an edge (s, v) with the weight $E(1,0) - E(0,0)$ or, otherwise, we define an edge (v, t) with the weight $E(0,0) - E(1,0)$. In a similar way for vertex v', if $E(1,1) - E(1,0) > 0$ we define an edge (s, v') with weight $E(1,1) - E(1,0) > 0$ or, otherwise, we define an edge (v', t) with the weight $E(1,0) - E(1,1)$. Fig. 1(a) shows an example where $E(1,0) - E(0,0) > 0$ and $E(1,0) - E(1,1) > 0$. Fig. 1(b) illustrates the complete graph obtained at the end.

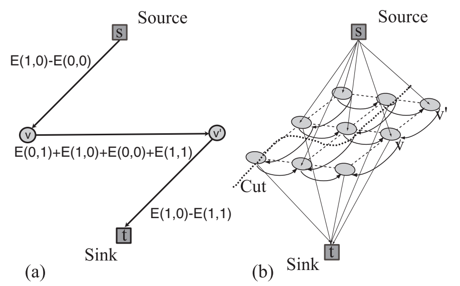

Fig. 1. (a) Elementary graph for a single energy term, where s and t represent source and sink respectively, and v and v' represent the two pixels involved in the energy term. In this case $E(1,0) - E(0,0) > 0$ and $E(1,0) - E(1,1) > 0$. (b) The graph obtained at the end results from adding elementary graphs.

As we have shown above, building on results from [6] and from [15], we can iteratively find an energy minimum through binary optimizations, based on max-flow calculation on a certain graph.

Algorithm 1 shows the pseudo-code for the Phase Unwrapping Max-Flow (PUMF) algorithm.

4. EXPERIMENTAL RESULTS

The results presented in this section were obtained by a MATLAB coding of the PUMF algorithm [max-flow was coded in C++ (see [17])].

Figs. 2(a) and 2(b) display two phase images to be unwrapped; they are synthesized from an original absolute phase surface formed by two equal size planes with slopes 0 and 1 rad/pixel (maximum height is 99 rad). The wrapped images are generated according to an InSAR observation statistics (see, e.g., [6]) with coherence 1.0 and 0.95, respectively. The wrapped phase image is then obtained, by computing the product of one image by the complex conjugate of the other, and finally taking the argument. The coherence value of 0.95 is low enough to induce a large number of phase jumps (*residues*), making the unwrapping a very difficult task. Figs. 2(c) and 2(d) show the corresponding unwrapped surfaces by PUMF with $p = 1$, both taking 16 iterations and, approximately, 4 seconds in a 2GHz PC. We can see that, even with low-coherence induced discontinuities, PUMF successfully accomplishes a meaningful unwrapping.

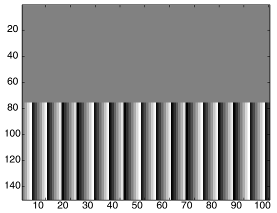

(a) Wrapped sheared planes. The correlation coefficient of the associated pair is $\alpha = 1.0$.

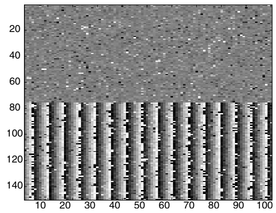

(b) Wrapped sheared planes. The correlation coefficient of the associated pair is $\alpha = 0.95$.

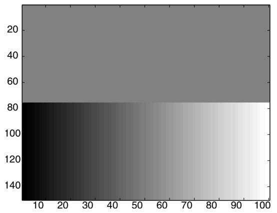

(c) Image in (a) unwrapped by PUMF with p=1.

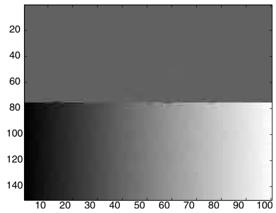

(d) Image in (b) unwrapped by PUMF with p=0.1.

Fig. 2. PUMF results for two sheared planes.

The Figs. 3(a) and 3(b) are analogous to 2(a) and 2(b), but now the original absolute phase surface is a Gaussian elevation with a height of 14π rad, and standard deviations $\sigma_i = 15$ and $\sigma_i = 10$ pixels; additionally in a quarter of the plane, the Gaussian has zero height introducing surface discontinuities, therefore rendering a quite difficult unwrapping problem. As is shown in Figs. 3(c) and 3(d), PUMF, using the 2π quantized L^p norm, correctly unwraps both surfaces with $p = 1$ and $p = 0.1$ respectively (taking 7 iterations).

Finally, to rank the PUMF algorithm, we applied the following algorithms to the above unwrapping problems:

- **Path following type:** Golstein's branch cut (GBC) [7]; quality guided (QG) [18]; and mask cut (MC) [19].
- **Minimum norm type:** Flyn's minimum discontinuity (FMD) [12]; weighted least-squares (WLS) [20]; and L^0 norm (L0N) (see [1, ch. 5.5]).

Path following and minimum norm algorithms were implemented with the code supplied in the book [1], using the following settings: GBC (-dipole yes); QG, MC, (-mode min_var -tsize 3); and WLS (-mode min_var -tsize 3, -thresh yes).

The PUMF algorithm achieves the best error norm in the four experiments. Its advantage is larger in the noisy scenario, where the error norms are 0.45 (PUMF), 23.6 (GBC), 36.4 (QG), 0.8 (FMD), 13.3 (MC), 39.0 (L0N), and 46.0 (WLS) for the sheared planes; and 0.4 (PUMF), 10.8 (GBC), 11.3 (QG), 11.6 (FMD), 5.2 (MC), 31.9 (L0N), and 21.7 (WLS), for the Gaussian elevation.

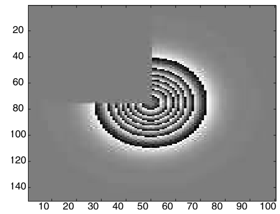

(a) Wrapped Gaussian elevation with a quarter of the plane with zero height. The correlation coefficient of the associated pair is $\alpha = 1.0$.

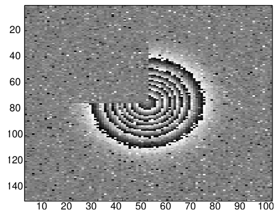

(b) Wrapped Gaussian elevation with a quarter of the plane with zero height. The correlation coefficient of the associated pair is $\alpha = 0.95$.

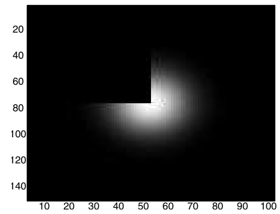

(c) Image in (a) unwrapped by PUMF with p=1.

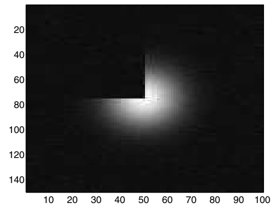

(d) Image in (b) unwrapped by PUMF with p=0.1.

Fig. 3. PUMF results for a Gaussian with a quarter of the plane with zero height.

5. CONCLUDING REMARKS

We developed a new graph cuts based phase unwrapping algorithm, in the vein of the minimum L^p norm class of PU algorithms, with $p \geq 1$. An iterative binary optimization scheme was adopted from $\mathbb{Z}\pi$M algorithm [6], and the results on energy minimization from [15] were applied, to perform the optimization, casting it on a series of graph max-flow/min-cut computations. Although we have not addressed the noise problem explicitly, PUMF is able to deal with discontinuities, in some cases even when their locations are unknown. In a set of experiments, the proposed PUMF algorithm outperforms state-of-the-art methods. The underlying reasons for the success of PUMF for $p < 1$ (with correspondingly enhanced discontinuities handling), is an issue to be addressed in the future. A more thorough benchmarking with existing phase unwrapping algorithms should also be performed as well.

The authors acknowledge Vladimir Kolmogorov for the max-flow/min-cut C++ code made available on the web.

6. REFERENCES

[1] D. Ghiglia and M. Pritt. *Two-Dimentional Phase Unwrapping. Theory, Algorithms, and Software*. John Wiley & Sons, New York, 1998.

[2] P. Rosen, S. Hensley, I. Joughin, F. LI, S. Madsen, E. Rodriguez, and R. Goldstein. Synthetic aperture radar interferometry. *Proceedings of the IEEE*, 88(3):333–382, March 2000.

[3] P. Jezzard and R. Balaban. Correction for geometric distortion in echo-planar images from B_0 field variations. *Magnetic Resonance in Medicine*, 34:65–73, 1995.

[4] S. Pandit, N. Jordache, and G. Joshi. Data-dependent systems methodology for noise-insensitive phase unwrapping in laser interferometric surface characterization. *Journal of the Optical Society of America*, 11(10):2584–2592, 1994.

[5] K. Itoh. Analysis of the phase unwrapping problem. *Applied Optics*, 21(14), 1982.

[6] J. Dias and J. Leitão. The $\mathbb{Z}\pi$M algorithm for interferometric image reconstruction in SAR/SAS. *IEEE Transactions on Image Processing*, 11:408–422, April 2002.

[7] R. Goldstein, H. Zebker, and C. Werner. Satellite radar interferometry: Two-dimensional phase unwrapping. In *Symposium on the Ionospheric Effects on Communication and Related Systems*, volume 23, pages 713–720. Radio Science, 1988.

[8] D. Ghiglia and L. Romero. Minimum L^p norm two-dimensional phase unwrapping. *Journal of the Optical Society of America*, 13(10):1999–2013, 1996.

[9] G. Nico, G. Palubinskas, and M. Datcu. Bayesian approach to phase unwrapping: theoretical study. *IEEE Transactions on Signal Processing*, 48(9):2545–2556, Sept. 2000.

[10] B. Friedlander and J. Francos. Model based phase unwrapping of 2-d signals. *IEEE Transactions on Signal Processing*, 44(12):2999–3007, 1996.

[11] D. Fried. Least-squares fitting a wave-front distortion estimate to an array of phase-difference measurements. *Journal of the Optical Society of America*, 67(3):370–375, 1977.

[12] T. Flynn. Two-dimensional phase unwrapping with minimum weighted discontinuity. *Journal of the Optical Society of America A*, 14(10):2692–2701, 1997.

[13] M. Costantini. A novel phase unwrapping method based on network programing. *IEEE Transactions on Geoscience and Remote Sensing*, 36(3):813–821, May 1998.

[14] J. Dias and J. Leitão. Simultaneous phase unwrapping and speckle smoothing in SAR images: A stochastic nonlinear filtering approach. In *EUSAR'98 European Conference on Synthetic Aperture Radar*, pages 373–377, Friedrichshafen, May 1998.

[15] V. Kolmogorov and R. Zabih. What energy functions can be minimized via graph cuts? *IEEE Transactions on Pattern Analysis and Machine Intelligence*, 26(2):147–159, February 2004.

[16] C. Chen. *Statistical-Cost Network-Flow Approaches to Two-Dimensional Phase Unwrapping for Radar Interferometry*. PhD thesis, Stanford University, 2001.

[17] Y. Boykov and V. Kolmogorov. An experimental comparison of min-cut/max-flow algorithms for energy minimization in vision. *IEEE Transactions on Pattern Analysis and Machine Intelligence*, 26(9):1124–1137, 2004.

[18] H. Lim, W. Xu, and X. Huang. Two new practical methods for phase unwrapping. In *Proccedings of the 1995 International Geoscience and Remote Sensing Symposium-IGARSS'95*, pages 196–198, Firenze, Italy, 1995.

[19] T. Flynn. Consistent 2-D phase unwrapping guided by a quality map. In *Proceedings of the 1996 International Geoscience and Remote Sensing Symposium-IGARSS'96*, volume 4, pages 2057–2059, Lincoln, NE, 1996.

[20] D. Ghiglia and L. Romero. Roboust two-dimensional weighted and unweighted phase unwrapping that uses fast transforms and iterative methods. *Journal of the Optical Society of America*, 11(1):107–117, 1994.